

STIMULATED TRANSFORMATIONS IN NANO-LAYERED COMPOSITES WITH $\text{Se}_{0.6}\text{Te}_{0.4}$

M. Malyovanik^a, M. Shipljak^a, V. Cheresnya^a, I. Ivan^{a,b}, S. Kokenyesi^{a,b*}, A. Csik^c

^aUzhgorod National University, Uzhgorod, Ukraine

^bUniversity of Debrecen, Debrecen, Hungary

^cATOMKI, Debrecen, Hungary

The influence of nanostructuring on the photo-thermostimulated structural transformations and related changes of optical, thermodynamical and electrophysical parameters were investigated in amorphous $\text{Se}_{0.6}\text{Te}_{0.4}$ films embedded into transparent SiO_x or As_2S_3 matrix. Namely comparison was made between homogeneous thin $\text{Se}_{0.6}\text{Te}_{0.4}$ films and $\text{Se}_{0.6}\text{Te}_{0.4}/\text{SiO}_x$ or $\text{Se}_{0.6}\text{Te}_{0.4}/\text{As}_2\text{S}_3$ -type nano-multilayer structures. It was established that crystallization and interdiffusion processes depend on the type of matrix in the nano-layered structure, what enables additional operation of the optical recording in this type of chalcogenide-based memory materials.

(Received January 10, 2005; accepted May 26, 2005)

Keywords: Amorphous chalcogenides, Nanostructures, Structural transformations, Memory effects

1. Introduction

The main types of the photo-induced structural transformations (PST) in chalcogenide glasses and amorphous layers can be systematized as i) structural transformations within amorphous phase, ii) photo-induced crystallization or amorphization, iii) photo-induced mass transport. These main known types of PST can be further detailed, for example concerning photo-induced anisotropy, photo-bleaching, etc., and are widely investigated (see for example [1-4]). But the fundamentals of these effects even in the most known compositions like AsSe , As_2S_3 are not clear, unambiguous, especially for the nanostructures, where the possible cluster formation [5], size restrictions and interface conditions may essentially influence the parameters of the material.

The basic applied problem related to the PST consists of the possibility of digital or analog optical information storage, phase change memory, fabrication of elements for optics and photonics. These applications require determined spectral and temperature range of functioning, increased sensitivity, transformation rates and stability of the memory at the same time. The realization of such requirements can be expected in nanosized objects made of chalcogenides due to the suitable change of thermodynamical parameters, conductivity, optical and other characteristics.

A few approaches are known for extending investigations of amorphous chalcogenide layers towards the nanostructures, especially the nanolayered, superlattice-like multilayer structures (MLS) [4,6-9], but the problem of PST dependence on the artificial nanostructuring is still not solved. Inserting the light-sensitive glass, for example the typical model one $-\text{Se}_x\text{Te}_{1-x}$ – into the dielectric matrix and changing the dimensions of these glass-elements, as well as the type of matrix, new effects are expected: stimulation of the solid-state reactions, crystallization, and the shift of optical absorption edge. Important data on crystallization kinetics in thin Ge-Sb-Te films sandwiched between transparent protective layers are presented in [10]. The enhanced interdiffusion in the $\text{a-Se/As}_2\text{S}_3$ nano-multilayers results in the giant volume expansion [11]. So other combinations of components in similar nano-composites should be realized and analyzed for the development of this type of metastable, memory materials. The establishment of correlations between the compositional modulation at nanoscale-dimensions ($\sim 3\text{-}10$ nm) in $\text{Se}_{0.6}\text{Te}_{0.4}$ – containing nanostructures, and the changes of the above mentioned optical and electrical parameters as well as the possible improvement of optical recording process in comparison with homogeneous $\text{Se}_{0.6}\text{Te}_{0.4}$ films were the aims of the present work.

* Corresponding author: kiki@tigris.klte.hu

2. Experimental

Bulk $\text{Se}_{0.6}\text{Te}_{0.4}$ composition can be considered good glass former [12] what promotes obtaining amorphous film, which in turn can be rather easily crystallized according to our experience. Thin films were prepared by thermal evaporation of milled $\text{Se}_{0.6}\text{Te}_{0.4}$ glass in vacuum onto a Corning glass or Si-wafer substrate. Multilayer composites were deposited onto the similar substrate in successive cycles of evaporation of $\text{Se}_{0.6}\text{Te}_{0.4}$ glass and of the matrix material from different sources. Matrix materials which serve as optically transparent barriers between the narrow band gap $\text{Se}_{0.6}\text{Te}_{0.4}$ were SiO_x or As_2S_3 . The periods of the compositional modulation Λ were in the 5 – 12 nm range, as determined from the Low Angle X-Ray Diffraction (LAXRD) and can be set by the deposition conditions (intensity of the vapor beams and the deposition time of each component). The total thickness of the multilayers, as well as of the separately deposited homogeneous films from the given components (0.5- 1.5 μm) was measured by optical methods.

Optical transmission was the main tool for measuring photo-(thermo) stimulated structural transformations which result crystallization. To clarify the interrelation between the transmittance change and crystallization X-ray diffraction and electron diffraction was measured as well as the surface roughening at nanometer scale which was determined by NT-MDT™ AFM or by scanning electron microscopy (SEM). DC conductivity was measured in a special vacuum chamber with a heated/cooled sample holder by a nanoamperemeter, on samples with in-plain geometry of carbon electrodes, which were deposited in two parallel scratches. The same chamber was used for the measurements of optical transmission. Structural transformation were induced by He-Ne laser radiation ($\lambda=0.63 \mu\text{m}$, output intensity 25 mW) focused into different size spots or by heating the sample, and optical transmission change was measured at the same wave-length by a weakened beam.

3. Results and discussion

The main result of our experiments consists in the demonstration of the influence of the matrix on the light- and thermo-induced crystallization in $\text{Se}_{0.6}\text{Te}_{0.4}$ which is embedded into this matrix and forms a layered nanocomposite. Crystallization occurs during heating or laser illumination in MLS, where the matrix (SiO_x) do not interact with chalcogenide material, whereas interdiffusion is prevailing in MLS, where the matrix (As_2S_3) interacts with $\text{Se}_{0.6}\text{Te}_{0.4}$ and solid solutions can be created before the crystallization develops.

Since the high crystallization ability of homogeneous $\text{Se}_{0.6}\text{Te}_{0.4}$ glass is known [13] it is not surprising, that a thin film, obtained during deposition from vapor onto the cold substrate and so initially amorphous can be easily transformed to the crystalline state either by direct heating up to the crystallization temperature or by irradiation. Electron diffraction experiments (Fig. 1) clearly confirm it. Essential surface roughening due to the crystallization was also proved by direct SEM and AFM investigations of the $\text{Se}_{0.6}\text{Te}_{0.4}$ surface.

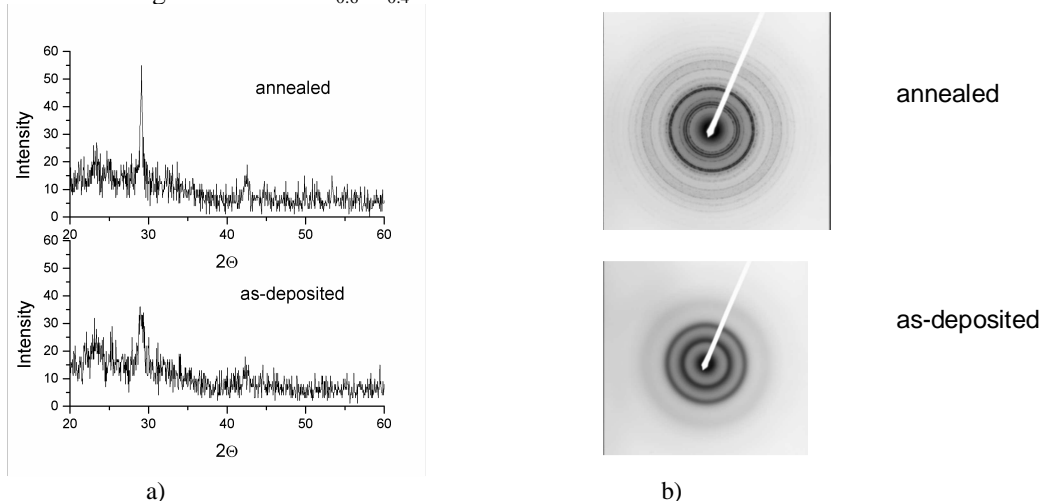


Fig. 1. a) X-ray diffraction spectra for initial and annealed $\text{Se}_{0.6}\text{Te}_{0.4}/\text{SiO}_x$ nanostructures, b) Electron diffraction picture for initial and crystallized $\text{Se}_{0.6}\text{Te}_{0.4}$ films.

Indirectly the crystallization was demonstrated on the temperature dependence of the electrical conductivity of as-deposited film (a breaking point near 356 K on curve 1, Fig.2 a). The layer became crystalline (curves 1' and 1''), the activation energy for the electrical conductivity decreases (see Table.1) and characterizes the crystalline state of the $\text{Se}_{0.6}\text{Te}_{0.4}$ composition. The same conclusion was made from the temperature dependence of optical transmission at $\lambda=0.63 \mu\text{m}$ (Fig.2. b, curve 1). The rather sharp decrease of the transmission correlates well with DC conduction change, so both effects can be used for determination of the phase change process in our thin film structures.

Table 1. Activation energies for electrical conductivity.

Material	E_a , eV (as deposited)	E_a , eV (annealed)
$\text{Se}_{0.6}\text{Te}_{0.4}$	0.85	0.38
$\text{Se}_{0.6}\text{Te}_{0.4}/\text{SiO}_x$	0.83	0.37
$\text{Se}_{0.6}\text{Te}_{0.4}/\text{As}_2\text{S}_3$	0.89	0.95

Only a rather high intensity He-Ne laser irradiation ($P \geq 10 \text{ W/cm}^2$ at the surface) causes optical transmission change (darkening) of such layer in an acceptable experimental time interval. At the same time darkening rate increases with additional heating of the sample (Fig. 3). It seems that the heating of the layer by irradiation may be important. But the same measurements at 190 K (Fig.4) demonstrate the essential role of the light in stimulated crystallization, even if irradiation intensity is enough for insignificant heating of the layer (the estimated $\Delta T \approx 8 - 14 \text{ K}$ for maximum intensity of irradiation). This effect follows also from the data presented in Fig.2.b.: the temperature threshold of the crystallization process decrease with increasing intensity of laser irradiation (curves 2', 2'', 2'''), partially because of the real temperature increase in the illuminated spot. More than that the shape of the curves (2- 2''') and the appropriate mechanism of the crystallization process change under irradiation. The transformation is irreversible, since during the successive cooling the transmission do not restores (see the almost horizontal dotted line in Fig. 2.b, curve 4), similarly to the conductivity of the thermally crystallized films (Fig. 2.a., dotted curves 1'' and 2'').

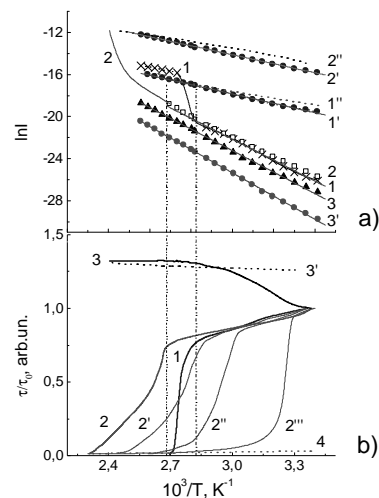


Fig. 2. a) The temperature dependence of the conductivity current in $\text{Se}_{0.6}\text{Te}_{0.4}$ films before the crystallization (1), during the cooling after annealing at 400 K (1') and the next heating (1''). The same for $\text{Se}_{0.6}\text{Te}_{0.4}/\text{SiO}_x$ MLS (2, 2', 2'', 2''') (annealing was performed at 430 K). For as-deposited $\text{Se}_{0.6}\text{Te}_{0.4}/\text{As}_2\text{S}_3$ MLS the conductivity follows curve 3 and for annealed one – the curve 3'); b) The temperature dependence of the optical transmission τ relative to the initial τ_0 at $\lambda=0.63 \mu\text{m}$ for $\text{Se}_{0.6}\text{Te}_{0.4}$ (1), $\text{Se}_{0.6}\text{Te}_{0.4}/\text{SiO}_x$ (2) and $\text{Se}_{0.6}\text{Te}_{0.4}/\text{As}_2\text{S}_3$ (3). Curves 2', 2'' and 2''' were measured under He-Ne laser illumination with intensities 3.5 W/cm^2 , 7.0 W/cm^2 , and 14 W/cm^2 correspondingly. Curves 3' and 4 characterize the transmission change during the cooling of the samples.

Activation energies for electrical conductivity correlate with the quasi-forbidden gap energy E_g^* for amorphous $\text{Se}_{0.6}\text{Te}_{0.4}$ in homogeneous layer and in multilayers, i.e. these are equal to $\approx 0.5 E_g^*$ determined from the slope of the optical absorption edge. Essential increase of E_a in annealed $\text{Se}_{0.6}\text{Te}_{0.4}/\text{As}_2\text{S}_3$ multilayer is obviously connected with formation of ternary As-S-Se-Te glass composition after the interdiffusion (such glasses are characterized by increased E_g^*). At the same time the activation energy is smaller for $\text{Se}_{0.6}\text{Te}_{0.4}$ crystalline material in comparison with amorphous one.

The dependence of optical transmission on time (weak control beam) or on illumination time (intense laser beam) at different temperatures (see the example for $\text{Se}_{0.6}\text{Te}_{0.4}$ in Fig.3.) was measured both for $\text{Se}_{0.6}\text{Te}_{0.4}$ films and $\text{Se}_{0.6}\text{Te}_{0.4}/\text{SiO}_x$ ML.

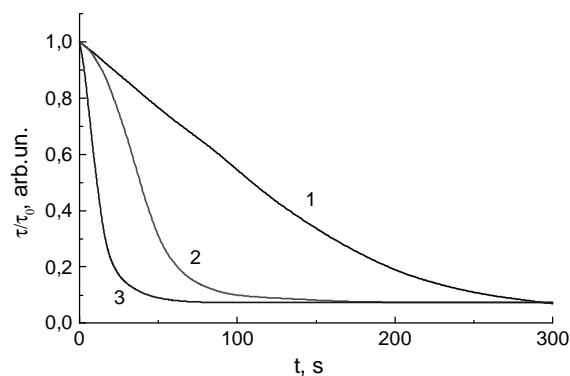


Fig. 3. The change of the optical transmission relative to the initial (τ/τ_0) at $\lambda=0,63 \mu\text{m}$ for $\text{Se}_{0.6}\text{Te}_{0.4}$ homogeneous thin film at different temperatures T of laser recording: 1 – $T=360 \text{ K}$, 2 – $T=373 \text{ K}$, 3 – $T=382 \text{ K}$.

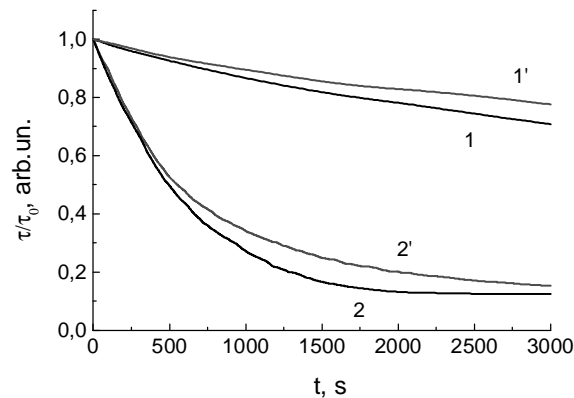


Fig. 4. The change of the optical transmission τ relative to the initial τ_0 at $\lambda=0,63 \mu\text{m}$ under the influence of He-Ne laser irradiation ($P=25 \text{ W/cm}^2$) in $\text{Se}_{0.6}\text{Te}_{0.4}$ film (1, 1') and $\text{Se}_{0.6}\text{Te}_{0.4}/\text{SiO}_x$ nanocomposite (2, 2'): 1, 2 – $T=290 \text{ K}$, 1', 2' – $T=190 \text{ K}$.

The results were used to determine the effective activation energies of crystallization $E_{ac,thermo}$ or $E_{ac,photo}$ as well as the reaction order n of the crystallization process using the well known Johnson-Mehl-Avrami formula, similarly to the analysis made in [10]:

$$x = 1 - \exp(-K \cdot t^n) \quad (1)$$

where x is the crystallized fraction, measured by the change of the optical density of the layer, K is the rate constant, t is the time required to reach the x state, and n is the reaction order. Since $K = B \cdot \exp[-E_{ac}/kT]$, where k is the Boltzmann's constant and B is a constant, E_{ac} can be determined and used together with n for the definition of the transformation process. The Avrami exponent n depends in a complex and ambiguous way on the nucleation and crystal growth, especially in a complex heterogeneous material, but in general it is expected that crystal grain growth dominates the process if n is in the range $1.0 - 1.3$ and $n \geq 1.5$ if grain growth occurs with nucleation [10,14,15].

For $1.5 \leq n < 2.5$ the decrease of the nucleation rate with a progress of the grain growth is assumed in Ge-Sb-Te amorphous thin layers sandwiched between dielectric layers [10].

Our experiments show that phase change process can be essentially influenced if the crystallizing glass is inserted into the matrix which limits its dimensions at least in one direction. Our $\text{Se}_{0.6}\text{Te}_{0.4}/\text{SiO}_x$ MLS most likely are composites, which consist of layers of $\text{Se}_{0.6}\text{Te}_{0.4}$ nanoclusters, surrounded by SiO_x matrix, since the LAXRD curves show only a rather small and wide first order diffraction peak according to the period $\Lambda = 8$ nm, which indicates rather rough interfaces in the layered structure.

Table 2. Parameters of thermo- and photo-stimulated crystallization.

Material	K, s^{-1} (photo, at T=293 K)	n (thermo)	n (photo)	E_{ac} , eV (thermo)	E_{ac} , eV (photo)
$\text{Se}_{0.6}\text{Te}_{0.4}$	$(1.1 \pm 0.1) \cdot 10^{-4}$	1.4	1.5	1.0 ± 0.1	0.7 ± 0.1
$\text{Se}_{0.6}\text{Te}_{0.4}/\text{SiO}_x$	$(9.7 \pm 0.1) \cdot 10^{-4}$	1.3	1.2	1.2 ± 0.1	0.6 ± 0.1

Experimental data, presented in Table 2 refer to the more dominant role of the crystalline grain growth and enhanced transformation rates in illuminated $\text{Se}_{0.6}\text{Te}_{0.4}/\text{SiO}_x$ MLS in comparison with single $\text{Se}_{0.6}\text{Te}_{0.4}$ layer. It is not surprising due to the definite presence of crystalline nuclei or even crystallites in as-deposited $\text{Se}_{0.6}\text{Te}_{0.4}/\text{SiO}_x$ MLS (fig.1, a), what in turn may be explained by the influence of heterogeneous nucleation at interfaces in the ready MLS as well as at the stage of MLS deposition, which includes a rather low-temperature evaporation of $\text{Se}_{0.6}\text{Te}_{0.4}$ (~640 K) and a high-temperature evaporation of SiO_x component (~1000 K). The shape of the curve 1 in Fig.2.b corresponds to the grain growth with nucleation in a single $\text{Se}_{0.6}\text{Te}_{0.4}$ layer, at decreasing nucleation rate with a progress of the transformation. Under increasing illumination intensity the character of such curves become very similar to the curves 2'', 2''' for $\text{Se}_{0.6}\text{Te}_{0.4}/\text{SiO}_x$ MLS, which indicates the increasing role of the additional fast nucleation and growth at the initial stage of the transformation up to the saturation of nucleus concentration and the following slower crystal grain growth. In spite of the presence of nuclei in as-prepared $\text{Se}_{0.6}\text{Te}_{0.4}/\text{SiO}_x$ such MLS is thermally more stable in comparison with a single layer (curves 1 and 2 in Fig. 2.b), what can be explained by a presence of additional stresses and size restrictions, which causes a shift of the phase change temperatures in nanostructures [16] and also by the surface reactivity and chemical affinity of the combined layers [10].

The role of the illumination consists first of all in the essential lowering of the activation energies of the structural transformations, i.e. in the stimulation of this process even without the heating, what is characteristic for amorphous chalcogenides [1-4], especially due to the so called photoplasticity and enhanced mobility of the structural elements under illumination [17].

So, making the initial state of MLS more stable with respect to the temperature in comparison with a single layer, we can get more fast switch at high illumination intensities in a steady state process. This effect may be used for the development of thin nano-multilayer phase-change memory element, which can be read-out either optically or electrically. It would be interesting to see the backward process of amorphization, but it needs special pulsed illumination and will be performed later on together with a pulsed recording process. The present results support the possibility of efficient operation of the recording efficiency by nano-structuring of the chalcogenide-based recording material.

The above mentioned analysis applies to the MLS which consist of immiscible components or to the MLS where the stimulated intermixing process is slower in comparison with phase transition. Otherwise the interdiffusion dominates the steady state transformation of the MLS, as it is typical for chalcogenide/chalcogenide structures like $\text{Se}/\text{As}_2\text{S}_3$ [7,8] and for our $\text{Se}_{0.6}\text{Te}_{0.4}/\text{As}_2\text{S}_3$ samples. Just for this reason the temperature dependence of the conductivity in this as-deposited sample was measured at a rather high heating rate (~ 4 K/min) and interdiffusion occurs mostly during the annealing at 430 K. The conductivity of the intermixed structure was measured afterwards (curve 3' in Fig. 2a). The stimulated intermixing of the adjacent nanometer-thick layers in such semiconductor MLS results in the formation of solid solution with a wider band gap, in the bleaching of the whole structure and in the change of the electric conductivity, etc.(see the Table 1 and Fig.2.a, b). The read-out of the recorded information in these structures also may be done either optically or electrically. Enhanced intermixing rate in such MLS in the regime of steady state illumination or heating by laser beam also makes these materials applicable for optical recording, fabricating special optical elements with phase modulation. The whole process is similar to the

Se/As₂S₃ system [7,8] except of the higher sensitivity at $\lambda=633$ nm (He-Ne laser) and in the nearest spectral region due to the more efficient light absorption by “active” Se_{0.6}Te_{0.4} component of the MLS and higher diffusion coefficients in comparison with Se in Se/As₂S₃ structure.

Additional aspects of similarity or differences of the phase change process in both types of MLS where size restrictions and interface conditions influence crystallization may be examined only in experiments with pulsed laser illumination, what will be the matter of further investigations.

4. Conclusion

Two types of nano-multilayers, namely Se_{0.6}Te_{0.4}/SiO_x and Se_{0.6}Te_{0.4}/As₂S₃ were investigated with respect to the thermo- or light-stimulated structural transformations, since they strongly differ by the possibility of intermixing or crystallization in a steady-state process of heating or laser illumination.

Photo- and thermo-stimulated crystallization of nanometer-thick Se_{0.6}Te_{0.4} films embedded into SiO_x matrix in the form of nano-multilayer structure were measured with optical transmission and electrical conductivity change. It was found, that the as-prepared Se_{0.6}Te_{0.4}/SiO_x structure contains crystallites which in a considerable extent determine the transformation due to the grain growth limited process. Illumination essentially enhances crystallization both in the single Se_{0.6}Te_{0.4} layer and in the Se_{0.6}Te_{0.4}/SiO_x structure, making the process more nucleation-dependent and fast what results in the higher efficiency of the stimulated transformation and optical recording in such a nano-layered structure.

Photo- and thermo-stimulated interdiffusion prevail in Se_{0.6}Te_{0.4}/As₂S₃ nano-layered structure what results in efficient intermixing of the adjacent nanometer-thick layers, in photo- and thermally induced bleaching and in the change of electrical conductivity due to the formation of the solid solution of chalcogenide components.

Acknowledgements

Authors are grateful to L. Daroczi for electron diffraction measurements. This work was supported by Hungarian-Ukrainian Cooperation Grant UK-2/02 and Hungarian OTKA Grants # T 046758 and D048594.

References

- [1] J. Singh, K. Shimakawa, *Advances in Amorphous Semiconductors*, CRC Press, (2003).
- [2] H. Jain, *J. Optoelectron. Adv. Mater.* **5**, 5 (2003).
- [3] K. Shimakawa, A. Kolobov, S. R. Elliott *Adv. in Physics* **44**, 475 (1995).
- [4] A. Kikineshi in „Physics and technology of thin films, IWTF 2003” World Scientific Publishing, 318-323 (2004).
- [5] M. Popescu, *J. Optoelectron. Adv. Mater* **6**, 1147 (2004).
- [6] D. Nesheva, I. P. Kotsalas, C. Raptis, E. Vateva, *J. Non-Cryst.Solids* **224**, 283 (1998).
- [7] M. Malyovanik, S. Ivan, A. Csik, G. Langer, D.L. Beke, S. Kökényesi, *J. Appl. Phys.* **93**, 139 (2003).
- [8] A. Kikineshi, M. Malyovanik, Y. Messaddeq, V. Pinzenik, M. Shipljak, D. L. Beke, *J. Non-Cryst. Solids* **338-340**, 561 (2004).
- [9] I. Honma, H. Hotta, K. Kawai, H. Komiyama, K Tanaka, *J. Non-Cryst.Solids.* **97-98**, 947 (1987).
- [10] N. Ohshima, *J. Appl. Phys.* **79** (1996) 8357.
- [11] V. Palyok, I. A. Szabo, D. L. Beke, Kikineshi, *Appl.Phys A* **68**, 489 (1999).
- [12] V. B. Brasil, E. Meyer, *J. Non-Cryst.Sol.* **348**, 7 (2004).
- [13] H. Z. Vinogradova, *Glass forming and phase equilibria in chalcogenide systems*, „Nauka”, Moscow, (1984) (in Russian).
- [14] T. H. Jeong, M. R. Kim, H. Seo, *J. Appl.Phys.* **86**, 774 (1999).
- [15] G. Ruitenber, A. K. Petford-Long, R. C. Doole, *J. Appl. Phys.* **92**, 3116 (2002).
- [16] M. I. Komnik, *Size Effects in Thin Metallic Films*, Moscow State University, (1986) (in Russian).
- [17] M. L. Trunov, V. S. Bilanich, *Thin Solid Films* **459**, 228 (2004).